Optical and Quantum Electronics (2023) 55:1095
https://doi.org/10.1007/s11082-023-05350-2

Comprehensive analysis of single and double gate organic phototransistor

Ishrat Bashir[1] · S. Intekhab Amin[1] · Lubna Majeed[1] · Zuber Rasool[1] · Sunny Anand[2]

Received: 20 April 2023 / Accepted: 28 August 2023 / Published online: 28 September 2023

Abstract
In this work, we have done the comparative analysis of Single Gate and Dual Gate pentacene-based organic phototransistors (OPT). The opto-electrical simulations were done using 2-D Silvaco TCAD ATLAS device simulator. The SG-OPT and DG-OPT were simulated to provide deeper insight into behaviour of the two from both device physics perspective and quantitative standpoints. We have conducted an evaluation of both OPTs on account of the various important performance parameters at different electrical and optical bias over a wide spectral range. Our results shows how these different configurational OPT designs can influence the essential performance parameters while observing the variations in drain current, Current density, Energy band Diagrams and the various essential performance parameters such as Responsivity, photosensitivity, spectral response, quantum efficiency etc.

Keywords Organic phototransistor · Organic semiconductor · ATLAS-2D · Photocurrent · Dark current · Traps · Pentacene

✉ S. Intekhab Amin
samin@jmi.ac.in

Ishrat Bashir
Ishratbashir00@gmail.com

Lubna Majeed
lubmaj234@gmail.com

Zuber Rasool
rasoolzuber3@gmail.com

Sunny Anand
sunnyanand.42@gmail.com

[1] Department of Electronics and Communication Engineering, JamiaMilliaIslamia, New Delhi 110025, India

[2] Department of Electronics and Communication Engineering, Amity University, Noida, Uttar Pradesh 201301, India

1 Introduction

After decades of significant development in the field of optoelectronics and optoelectronic systems mostly photodetectors Depending on the applications, photosensors are used everywhere from industrial to commercial applications. However, most of these sensors consist of conventional inflexible inorganic semiconductors which limit their demand in today's world of wearable and flexible electronics. With the advent of IoT, the demand for economical, flexible, wearable, lightweight, low-power consumption sensors is growing rapidly. To meet all such demands, the cross-disciplinary research field of Organic electronics has paved a way for the following generation in offering simplistic processing and innovative and conformal substrate integration for a variety of applications (Nishide and Oyaizu 2008; Yamashita 2009; Hu et al. 2010; Kim et al. 2011; Salvatore et al. 2014; Chou et al. 2015; Hwang et al. 2015).The most studied and investigated devices in Organic optoelectronics are photodetectors which include organic phototransistors(OPT's) and organic photodiodes(OPD'S). Since organic transistors are considered to be an alternative to inorganic transistors. Notably organic field effect transistors (OFETs) are the prevailing subject of R&D right now due to their remarkable advantages compared to inorganic-based transistors.The OFET-based sensors are anticipated to have widespread applications from flexible displays, optical imaging, artificial skin, ecological monitoring, food safety detection, medication delivery, and medical diagnostics to high-performance biodegradable sensors (Someya et al. 2010; Torsi et al. 2013; Yu et al. 2013; Ren et al. 2021).

The organic phototransistor is a combination of a photodetector and an amplifier that has the ability to detect and convert an incident optical signal into an electrical signal, along with the amplification of the signal. As it is the combination of a photodetector and an amplifier it makes a viable applicant to be used in a wide range of optoelectronic applications, especially in the field of imaging where light detection and signal amplification plays a key role. Moreover, Organic phototransistors withfield-effect transistor geometry are extensively studied as they could be integrated into huge area circuits with higher densities as compared to BJT (Baeg et al. 2013; Noh et al. 2005). Like MOSFET, an Organic phototransistor with OFET geometry is a three terminal electrical device with source, drain and gate terminals but here instead of using inorganic semiconductor, we have photoactive organic semiconductor material and its resistance and conductance can controlled by Gate bias and light radiation (Ren et al. 2021; Baeg et al. 2013).

Under Dark conditions, on application of lateral external electric field across source-drain terminals, the current flows through the organic semiconductor referred as dark current. However this current can be further modulated by the applied gate voltage only (Tavasli et al. 2022).Under illumination conditions, when the energy of irradiance is made equivalent or higher than the forbidden energy gap of photoactive organic semiconductors, there happens to be the generation of electrons and holes with the large electrostatic force of attraction between them. These confined electrons and holes are known as excitons. These excitons will diffuse through the bulk of this organic semiconductor channel and with the application of an external electric field these excitons will undergo dissociation and thus creates free electron and hole carriers in the channel which are then collected at source-drain terminals and thus a significant amount of photocurrent will flow through the organic channel(Ren et al. 2021; Baeg et al. 2013; Tavasli et al. 2022).

Upon illumination, the operation of an OPT can be divided into two modes; Photovoltaic mode and photoconductive mode.

In Photovoltaic mode applied $V_{GS} < Vth$ (for P-Type) and OPT is in "ON state" (Accumulation Mode), the photo-generated electrons and holes in presence of lateral electric field gets accumulate under source and drain electrodes respectively which lowers the potential barriers across the electrodes and photoactive semiconductor that effectively reduces the contact resistance and induces a shift in Vth (Sangeeth et al. 2010). Thereby a substantial amount ofphotocurrent will flow through the organic channel. The logarithmic relationship defines the dependence of Photocurrent due to photovoltaic effect and light irradiance is expressed in Eq. (1);

$$I = \frac{AKT}{q} ln\left(1 + \frac{\eta qPopt}{Idarkhc}\right) \tag{1}$$

A is a proportionality parameter,k is the Boltzmann constant, η is the photo-generation quantum efficiency, hc/λ is the photon energy (Ren et al. 2021; Baeg et al. 2013; Tavasli et al. 2022).

In photoconductive mode applied Vgs > Vth (for p-type) and OPT is in "off state" and works in depletion mode, the photo-generated electrons and holes are responsible for the photocurrent in the device. Here only the light bias is responsible for modulating the current. Moreover, with an increase in optical intensity, the drain current increases linearly. In photoconductive mode, photocurrent is expressed by Eq. (2);

$$I = \left(q\mu_p pE\right)WD = BP_{opt} \tag{2}$$

Here B is a proportionality constant.

In addition to the specific OFET characteristics, the most important figures of merit that characterize the performance of an OPT are its Photoresponsivity, photosensitivity, External quantum efficiency, and spectral range. Photosensitivity (P) is defined as the ratio of photo-generated current to dark current and is expressed by Eq. (3) (Li et al. 2019). i.e.,

$$P = \frac{Ilight - Idark}{Idark} \tag{3}$$

Responsivity (R) is the measure of how efficiently a responsive photodetection takes place whenever exposed to light Intensity. It is determined by the ratio of generated photocurrent in the device to the incident power of irradiances given in Eq. (4) (Chow and Someya 2020). i.e,

$$R = \frac{Ilight - Idark}{Popt} \tag{4}$$

where Popt is incident optical power.

And External quantum efficiency (EQE) is the ratio of the number of photo-generated carriers to the number of incidentphotons in the device. It determines the efficiency associated with both light capturing and light conversion capabilities of the device and is expressed by Eq. (5) (Chow and Someya 2020). i.e.,

$$\mathrm{EQE} = \mathrm{R}\left(\frac{\mathrm{hc}}{\lambda \mathrm{q}}\right) \tag{5}$$

where R is Responsivity.

There are a lot of experimental studies on OPTs in the literature that is mostly concerned with analyzing the functionality of these devices. Different synthesis techniques, different semiconductors, and gate insulators with variable mobilities have all been claimed to increase the performance of existing devices. The organic semiconductor used in OFET-based OPT should have exceptional light-absorption capabilities, great carrier generation efficiency across a broad spectral range, and good mobility (Ren et al. 2021; Baeg et al. 2013; Liguori et al. 2016). Additionally, the materials of gate insulators and organic semiconductors are crucial to how well they work. Charge buildup and charge transport in the device are mainly influenced by different gate insulator parameters like dielectric constant and thickness (Lee et al. 2014; Sirringhaus 2005).P-type photoactive organic semiconductor pentacene is primarily explored since it possesses the necessary characteristics. Moreover, Pentacene's photosensing characteristics gets influenced by the dielectric/semiconductor interfacial traps and it has been observed thinner the gate oxide better the photosensitivity. Pentacene performs better under illumination when its thickness is reduced (Liguori et al. 2016). From the prespective of device architecture in order to increase the photodetection and sensitivity, several device designs, such as dual gate, vertical Organic Phototransistors, are being researched. Even though layered OPTs have made considerable strides, wide channel lengths prevent many excitons from effectively dissociating and even due to short exciton diffusion lengths which results in poor charge collection and the performance of OPT becomes limited. Since, a novel dual gate phototransistor device idea with a bulk heterojunction was described, in which both gates could accumulate and deplete both types of charge carriers to produce conductive n- and p-type channels at the gate's dielectric-semiconductor interface. As a result, high gain and linear photoresponse may be accomplished concurrently without the need of any additional circuitry (Chow et al. 2018). In order to improve the device performance vertical OPTs with shorter channel lengths are employed (Chen et al. 2020).As the electrical behaviour of an OFET is greatly influenced by the material utilised for the organic semiconductor thin film, channel length, and its thickness. With respect to various architecture configurations, the influence of channel length modification on device performance parameters has been demonstrated using Slivaco TCAD Atlas (Mittal et al. 2012). Furthermore, a comparative analysis of various architectural designs of OFETs has been investigated (Bhargava et al. 2015). All the above investigations were taken into consideration before carrying out all the optoelectrical simulations.In this work, our main aim is to study and compare the performance of OPT from the perspective of device configuration and provide deeper insight into behaviour of the device from physics perspective and various quantitative standpoints.

2 Simulation set up

The numerical and optoelectrical simulations of the schematic SG-OPT and DG-OPT are carried out by using TCAD ATLAS 2-D device simulator. We have used 2-D Luminous optical device simulator for illuminating the device. It equipped the simulated structures with light irradiances of different spectral wavelengths and of different beam intensities. To precisely determine the rate of photo absorption and photo generation at defined meshes, we employed the Ray Trace method. Moreover we have employed biomolecular LANGEVIN Recombination model as optical model. While FLDMOB, HOPMOB, PFMOB are used for the transportation of carriers in the devices. The fldmob accounts for the mobility of charge carriers when applied with the electric field and Poole frenkel mobility and

hopping mobility models accounts electron hole mobility associated with the organic semiconducting materials. Moreover the Poole–Frenkel model accounts for the conduction of trap-assisted carriers. In this study we have incorporated the interface traps into simulations so the non-radiative trap-assisted recombination is accounted by Shockley Read–Hall (SRH) recombination model.The schematic cross-sectional view of a Single Gate and Dual gate Pentacene based Phototransistor is shown in Fig. 1a and b respectively.

Pentacene is mostly employed P-type organic semiconductor because of its excellent light absorption properties and great carrier generation efficiency over a wide spectral range. The SG-OPT is based on typical bottom gate bottom contact organic field effect transistor configuration.It consists of an Aluminium layer of thickness 20 nm used as a gate electrode. A high K dielectric titanium dioxide layer is used as a gate insulator and it is 12 nm thick. Whereas the gate insulator is stacked with a 150 nm thick organic photosensitive semiconductor layer of Pentacene. Moreover, the 50 nm thick gold is placed as the source and drain electrodes as shown in the Fig. 1a. The channel length of SG-OPT is 20 µm and the channel width is of 1 mm.For Dual gate OPT, we have stacked our SG-OPT with transparent secondary gate oxide TiO_2 and onto which a transparent Indium Tin oxide (ITO) is used as top gate as shown in Fig. 1b, device dimension parameters and materials of SG OPT and DG-OPT has been mentioned in Table 1. The ITO and secondary gate oxide TiO_2 are transparent to make sure the photo absorption behavior of the DG-OPT is due to photoactive Pentacene only. In this configuration, we are considering the bottom gate as our primary gate and top gate as secondary gate. The device length for both the devices is 40 µm. Various parameters used in the 2-D opto-electrical simulation of SG-OPT and DG-OPT is given in Table 2.

Both the single gate and dual gate organic phototransistors are illuminated using monochromatic source, which is placed just few nanometers above them. The photoactive pentacene region is directly exposed to the optical radiation in SG-OPT while in DG-OPT the optical radiations are coupled into the device through the transparent ITO and TIO_2 and

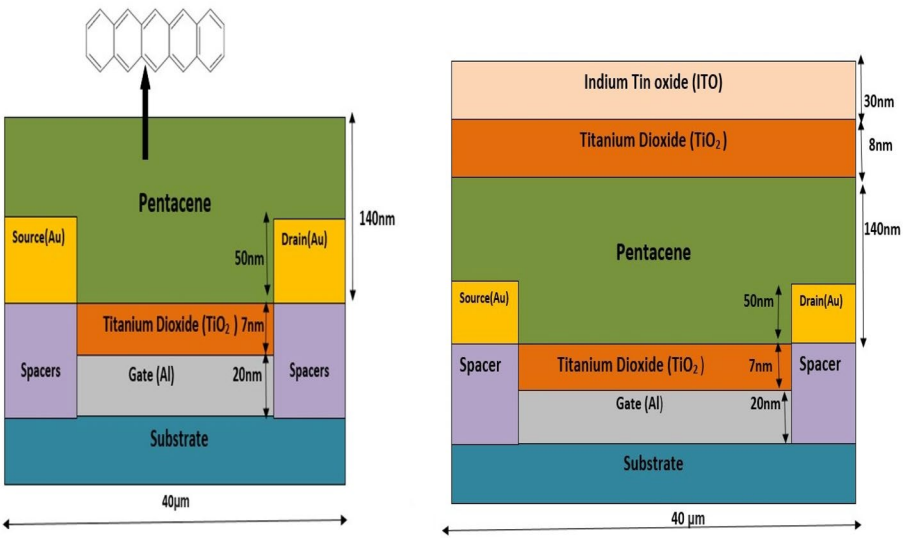

Fig. 1 **a** and **b** showing the schematic cross-sectional view of a single gate and dual gate pentacene based phototransistor

Table 1 Device dimension parameters and materials of SG OPT and DG-OPT

Parameter name	Material	Value
Primary (bottom) gate thickness	Aluminium	20 nm
Primary(bottom) gate oxide thickness	TiO_2	7 nm
Channel thickness	Pentacene	140 nm
Channel length		20 µm
Channel/device width		1 µm
Secondary (top) gate oxide Thickness	TiO_2	8 nm
Secondary (top) gate thickness	ITO	30 nm
Source thickness drain thickness	Gold	50 nm 50 nm

Table 2 Various parameters used in the 2-D opto-electrical simulation of SG-OPT and DG-OPT

Material	Parameter	Value
Pentacene	Ionization potential	5.2 eV
	Electron affinity	2.8 eV
	Dielectric constant	3.6
	Hole mobility	$0.85 cm^2/v^{-s}$
	Band gap energy at 0 K	2.2 eV
TiO_2	Permittivity	80
Gold	Work function	5.1 eV
Aluminium	Work function	4.1 eV
	Permitivitty	9

modulates the electrical characteristics of the device. The ITO and secondary gate oxide TiO_2 are transparent to make sure the photo absorption behavior of the DG-OPT is due to photoactive Pentacene only. The amount of light absorption associated with the thickness (140 nm) of Pentacene is mainly measured with absorption coefficient (α) and the real refractive index (n) and imaginary refractive index (k) helps the simulator to calculate the absorption capability of the material at specific wavelengths as mentioned in Table 3.

3 Results and discussion

3.1 Under dark

To understand the basic operation and characteristics of simulated SG pentacene OPT based on BGBC configuration and DG Pentacene based OPT, the transfer and output characteristics were measured in the dark at various bias conditions. By reproducing the results obtained experimentally in (Klauk et al. 2007), calibration of the simulation parameters has been carried out in order to match the characteristics as shown in Fig. 2.

Under dark conditions, both the OPT's showed typed typical p-Type transistor behaviour, the output characteristics shows variation of drain current I_{DS} and drain voltage $V_{DS,}$ while V_{DS} is sweeped from 0 to − 40 Volts and gate voltage $V_{DS,}$ is kept constant − 10, − 20, − 30, − 40 Volts as shown in Fig. 3. Furthermore transfer characteristics shows the variation of of drain current I_{DS} and gate voltage V_{GS}, when V_{GS} is varied from 0 V to − 40 V and Drain Voltages V_{DS} is kept constan t − 10 V, − 20 V, − 30 V, − 40 V are

Table 3 Real and imaginary refractive index values of ITO,TiO_2 and pentacene used in opto-electrical simulation of both the OPTs and their corresponding absorption coefficient for various incident wavelengths

ITO			TiO_2		Pentacene		
Wavelength (λ) (um)	n_1	K	n_1	k	n_1	K	α (cm^{-1})
0.3	2.311889	0.102267	4.6501057	0	1.4625	0.072855	26,157.798
0.35	2.2139858	0.0594361	4.5405688	0	1.4625	0.072855	26,157.798
0.4	2.119688	0.043934	3.3009565	0	1.54	0.062705	19,699.357
0.45	2.0408053	0.0405663	3.1423477	0	1.535	0.1151725	32,162.229
0.5	1.9771792	0.0427706	3.0357576	0	1.48	0.25212	63,364.667
0.55	1.926192	0.0475047	2.9587547	0	1.615	0.3187475	72,827.258
0.6	1.8851634	0.05329	2.9031818	0	1.645	0.41746	87,432.618
0.63	1.8630881	0.0571853	2.8757121	0	1.678	0.446349	88,749.794
0.65	1.8518767	0.0593878	2.8635606	0	1.705	0.5029275	97,230.359
0.68	1.8348874	0.063033	2.8416572	0	1.835	0.308435	56,998.655
0.7	1.8246125	0.0654273	2.8319697	0	1.95	0.08251	14,812.161

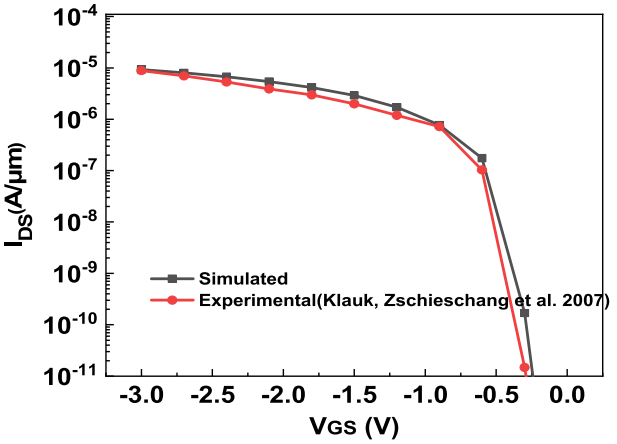

Fig. 2 Under dark conditions, comparison of published experimental data (Klauk et al. 2007) for OFET with a simulation result for the characteristics of the drain current (I_{DS}) and gate voltage (V_{DS})

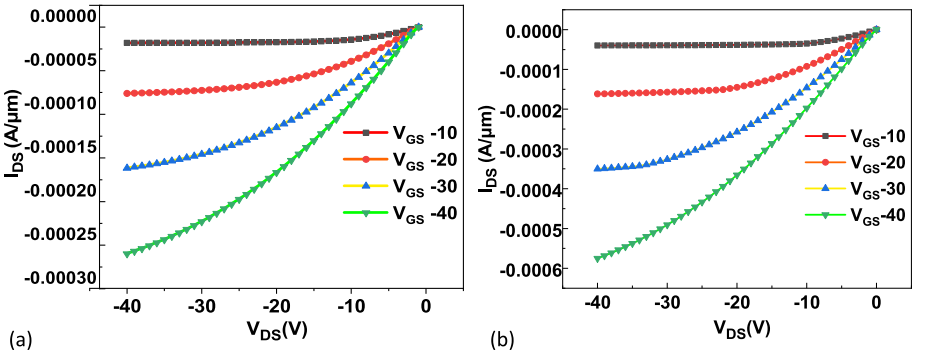

Fig. 3 Under dark conditions, Drain current versus drain voltage at different Gate bias **a** single gate **b** dual gate pentacene based OPT

shown in the Fig. 4. Moreover in DG-OPT we have applied symmetric bias to both primary and secondary gate.

The device operation of DG-pentacene-based OPT is the same as that of SG-OPT. Though the dual gate is responsible for modulating the channel carriers from both top and bottom sides. The outcomes of these results show that a DG-OPT's outperforms a SG-OPT in terms of performance. The observed results shows the dual-gate OPTs effectiveness with large drain output current at only modest operational voltage, enhanced channel controllability, larger field-effect mobility. A dual-gate consisting of a top and a bottom OPT, has two conduction channels and possibly twice as much the SG OPT. By applying an electric field over a channel with two transistor gates, the channel's electrical properties can be modified. Other than this the insulator oxide on two sides help in trapping of minority carriers at the semiconductor and insulator interface which further influences the characterisation of DG OPT. With applying symmetric bias of − 40 V to both the primary and the secondary gate, the channel carriers were modulated more than the SG-OPT which resulted in the rise in current density within the channel. From the fig it is quite clear that under dark, on-current of DG OPT is 0.6 mA which nearly double the value of 0.3 mA of SG-OPT. Furthermore, the characteristics of simulated SG OPT shows the resemblance with the experimental results at the mentioned bias conditions (Noh et al. 2005). DG device reduces the resistance of the channel by 50% percent by modulating the channel carriers from both the sides.

3.2 Under illumination conditions

The performance of the phototransistor is valued by different parameters and some of the underlying parameters are discussed in this section below: The energy band diagrams of SG-OPT and DG-OPT helps us with the proper understanding and illustration of the device operation in both dark and light bias.

The Occurence of band bending in the aforementioned diagrams is due to applied lateral electric field and the condition that assist modulation the charge carriers in an organic semiconductor channel i-e gate bias and light bias conditions. The variation of energy band for SG-OPT and DG-OPT is obtained by taking a cutline at 1 nm above the primary gate dielectric and channel interface, the extracted energy levels of HOMO and LUMO for various conditions are given in Fig. 4.

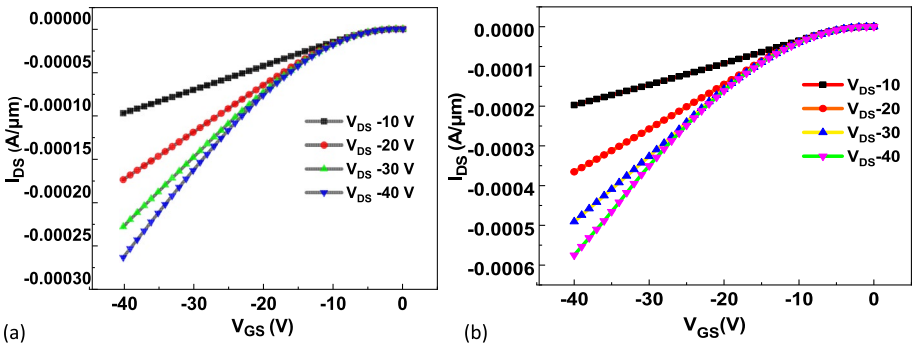

Fig. 4 Under dark conditions, drain current versus gate voltage at different drain bias is shown in a linear scale **a** SG-OPT **b** DG-OPT

It is quit evident from Fig. 5a and c when SG-OPT and DG-OPT is applied with lateral electric field Vds = -40 under dark conditions and no gate bias is applied. As Vgs = 0 and Vgs > Vth (− ve for p type) so this device is working in off state. Initially present positively charged holes in pentacene will start moving from source to drain terminal. And there are insufficient mobile carriers present at the condition.

Clearly from the bending diagrams,it is quit evident that on application of monochromatic light bias of 1W/cm^2,there happens to be photogenerated excitons that will dissociate into free electrons and holes due to applied laterial electric field due to Vds = − 40 V.The holes,which are more resistant to trapping events than the electrons, directly contribute to available photocurrent whereas the electrons gets trapped at the semiconductor/ dielectric interface by defects present there.There is enough bending in HOMO LUMO levels of both the devices to allow the conduction even in off state Vgs = 0. It can be observed from Fig. 5a & c the DG-OPT is showing steeper slope in bending upto the 30 eV at vgs = 0,whereas in SG-OPT slope is steeper upto 10 eV. The steeper bending can be credited to the presence of the secondary gate oxide layer and defects near the semiconductor/ dielectric interface. The traps alter the energy level alignment which assists in the dissocation of excitons and

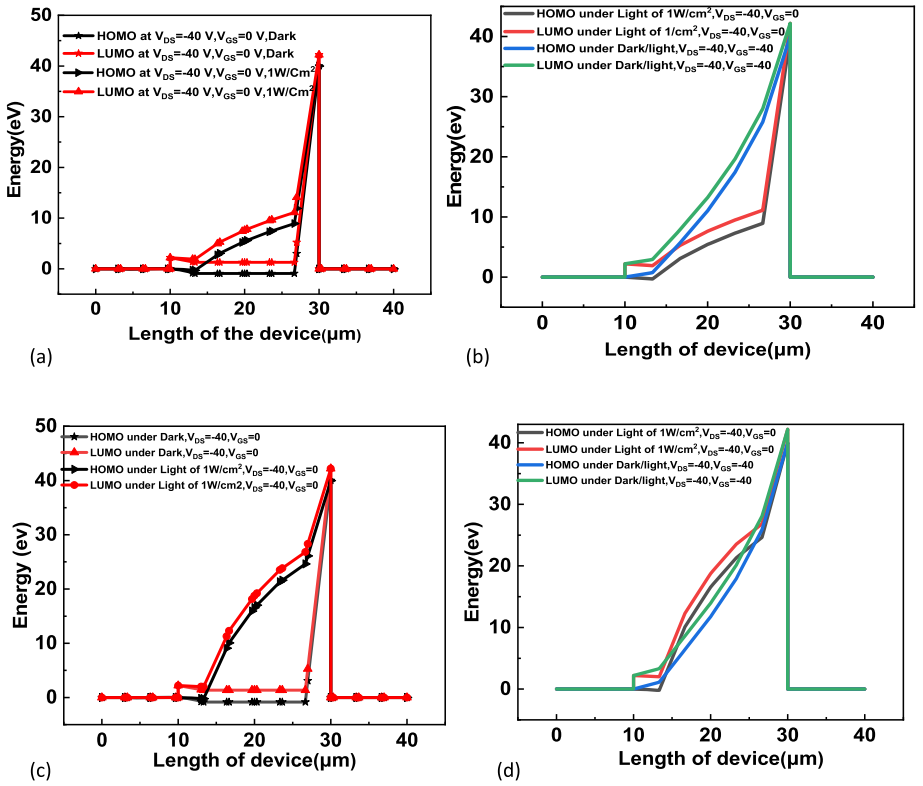

Fig. 5 The band diagram of **a** SG-OPT under dark and and monochromatic irradiation of 650 nm wavelength with intensity of 1W/cm^{2}Vgs = 0 V **b** SG-OPT under dark and monochromatic irradiation of 650 nm wavelength with an intensity of 1W/cm^2 at Vgs = 0 V and Vgs = − 40 V respectively **c** DG-OPT under dark and and under monochromatic irradiation of 650 nm wavelength with intensity of 1W/cm^{2}at Vgs = 0 V **d** DG-OPT under dark and monochromatic irradiation of 650 nm wavelength with intensity of 1W/cm^{2}at Vgs = 0 V and Vgs = − 40 V respectively

also helps with the trapping of minority carriers and thus increases the hole photo current in the device (Haneef et al. 2020).From Fig. 5b & d the band bending increases with the increase in the gate bias. Both devices exhibit sufficient bending to permit conduction due to light bias even in the off state but the current density in off state is very low in both SG-OPT and DG-OPT as compared to when gate bias is applied as shown in Fig. 6.

In Fig. 6 we have 2D contour plots of a SG and DG Pentacene based OPT showing current density when exposed to monochromatic irradiance of intensity 1W/Cm^2. Figure 6a & c shows when no gate bias is applied and both OPT's are in off state, the current density in both the devices is wholly due to the photo-generated carriers but the available photocurrent density of DG-OPT is large as in comparison to SG-OPT current density. In Fig. 6b & d, with the application of gate bias of − 40 V, OPT operates in accumulation mode the drain current increases exponentially with increase in drain bias however sensing of light is notably observed in off state only as the light bias current density is very small as compared to the gate bias current density to show its effect in on state. Thus our devices show domination of photoconductive effect over Photovoltaic effect.So in our further observations we have taken photoconductive behavior of the devices into consideration. The observed

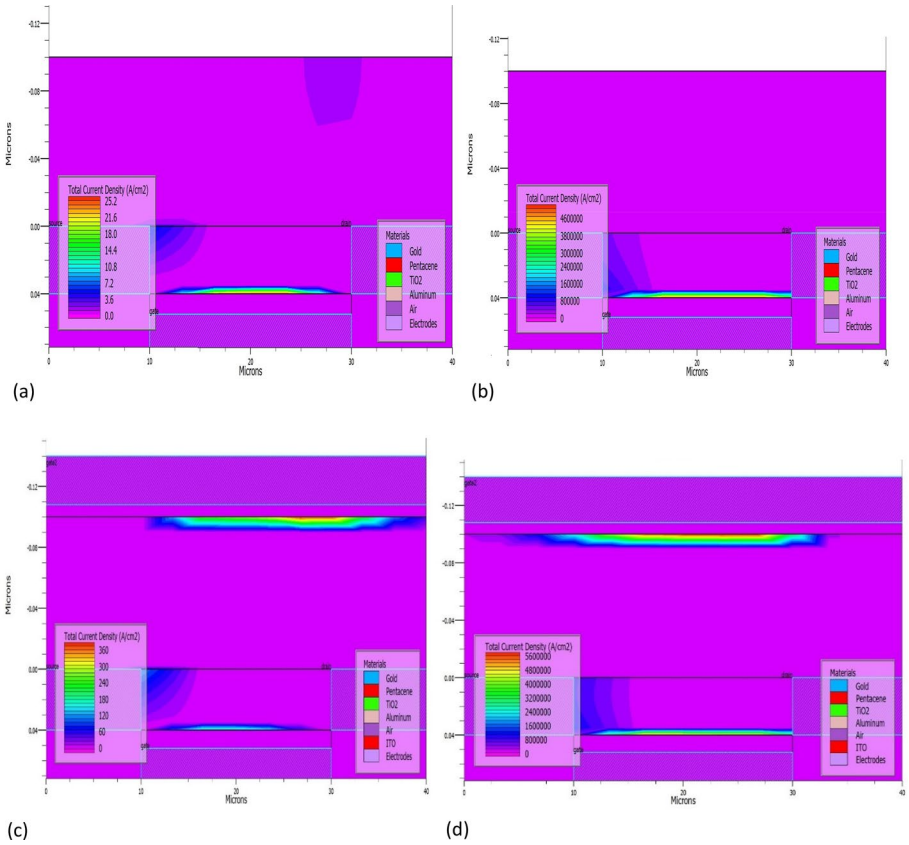

Fig. 6 The current density contour plots when exposed to monochromatic irradiation of 650 nm with intensity of 1W/Cm^2 **a** SG-OPT at no gate bias **b** SG-OPT when Vgs = − 40 V **c** DG-OPT at no gate bias **d** DG-OPT when Vgs = − 40 V

current density of DG-OPT is 160(A/cm^2) whereas it is 20(A/cm^2) for SG-OPT. The current density distribution along the channel when both the OPT's are exposed to monochromatic irradiation of 650 nm wavelength when no gate bias conditions is given in the Fig. 7.

In Fig. 6 we have 2D contour plots of a SG and DG Pentacene based OPT showing current density when exposed to monochromatic irradiance of intensity 1W/Cm^2.Fig. 6a & c shows when no gate bias is applied and both OPT's are in off state, the current density in both the devices is wholly due to the photo-generated carriers but the available photocurrent density of DG-OPT is large as in comparison to SG-OPT current density. In Fig. 6b & d, with the application of gate bias of − 40 V, OPT operates in accumulation mode the drain current increases exponentially with increase in drain bias however sensing of light is notably observed in off state only as the light bias current density is very small as compared to the gate bias current density to show its effect in on state. Thus our devices show domination of photoconductive effect over Photovoltaic effect.So in our further observations we have taken photoconductive behavior of the devices into consideration. The observed current density of DG-OPT is 160(A/cm^2) whereas it is 20(A/cm^2) for SG-OPT. The current density distribution along the channel when both the OPT's are exposed to monochromatic irradiation of 650 nm wavelength when no gate bias conditions is given in the Fig. 7.

3.2.1 Device characteristics under illumination

The output characteristic of both the OPT's were measured under the illumination of a monochromatic source with a wavelength of 650 nm at various beam intensities such as 1×10^{-3}W/cm^2, 1×10^{-2}W/cm^2, 1×10^{-1}W/cm^2, 1W/cm^2 at zero Gate bias, when drain voltage V_{DS} is sweeped in steps from 0 to − 40 V as shown in the Fig. 7. As our OPT's are notably photosensitive in (depletion mode) off state so we have simulated the drain characteristics under illumination at no gate bias condition. Figures 8a and b, It is evident that the in depletion mode, drain current increases with the increase in incident light intensity. In addition, the drain current value of the simulated DG-OPT is 2×10^{-8}, which is substantially higher than 1.6×10^{-9} of SG-OPT.

Moreover it is crucial to note that the output characteristics lacked the typical linear regime followed by a saturation regime. As the photo-generated carriers aren't enough to

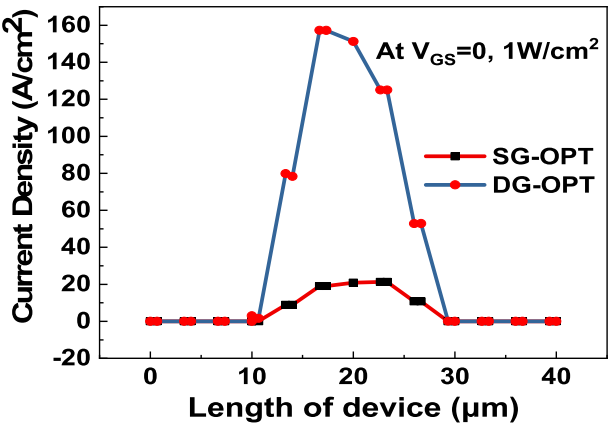

Fig. 7 Current density distribution of SG-OPT and DG-OPT along the channel under the monochromatic irradiation of 650 nm of 1W/cm^2 intensity

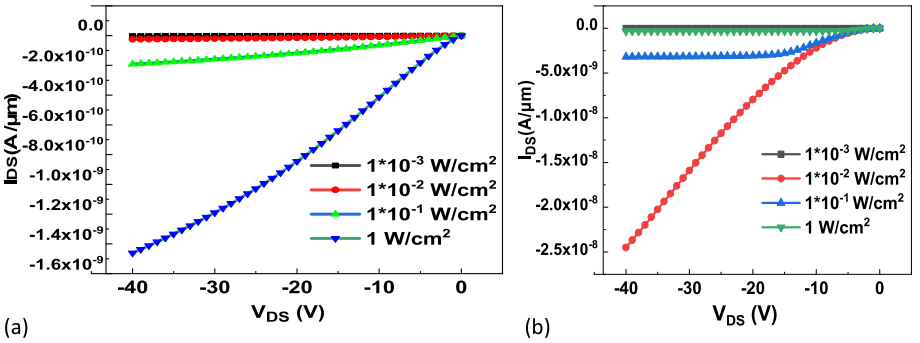

Fig. 8 Output characteristic showing drain current versus drain voltage when applied with monochromatic light bias of different intensities with 650 nm wavelength at no gate bias condition **a** SG-OPT **b** DG-OPT

make the channel go into pinch off state. So, no saturation state curve can be seen in this condition. Likewise the same trend has been observed in the work (Bhargava et al. 2015). We studied our simulated single gate and dual gate pentacene based-OPT under both the accumulation and depletion modes in both dark and illumination conditions.

Figure 9a and b shows the transfer characteristics of SG-OPT and DG-OPT at different beam intensities when VGS > -1 V the photo-generation of carriers are responsible for the increase in the carrier density in the device. With increase in optical flux the off state current increases in both the devices as the similar trend has been observed in the work (Bhargava et al. 2015). In addition, the off state drain current value of the simulated DG-OPT is substantially higher than that of the SG-OPT though the thickness of photosensitive organic semiconductor pentacene is same in both the devices. The drain current value of DG-OPT is of order 10^{-7} and SG-OPT is in order of $10^{-8}$when vgs = 0. The presence of secondary gate oxide and the traps associated with semiconductor and dielectric interface, increases the efficiency of the DG-OPT. However traps are usually

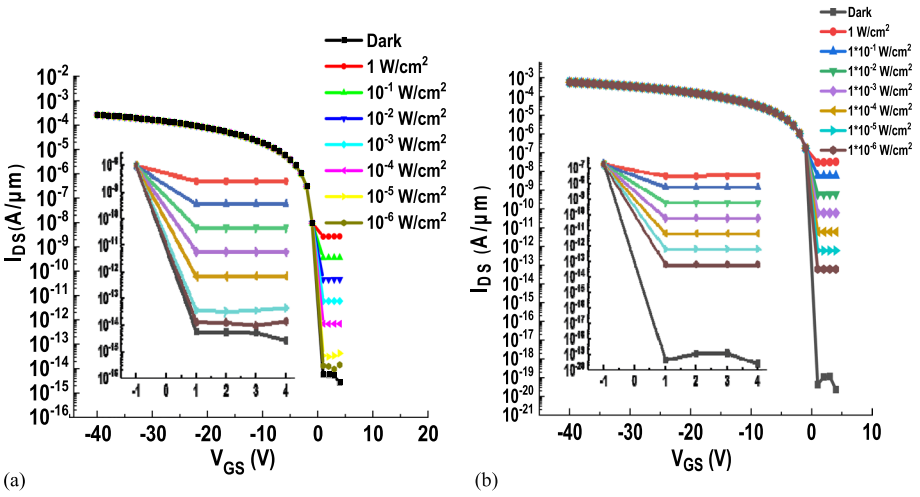

Fig. 9 **a** and **b** showing the variation in drain current versus gate voltage at constant Vds of − 40 V and at different light bias with wavelength of 650 nm in SG-OPT and DG-OPT respectively

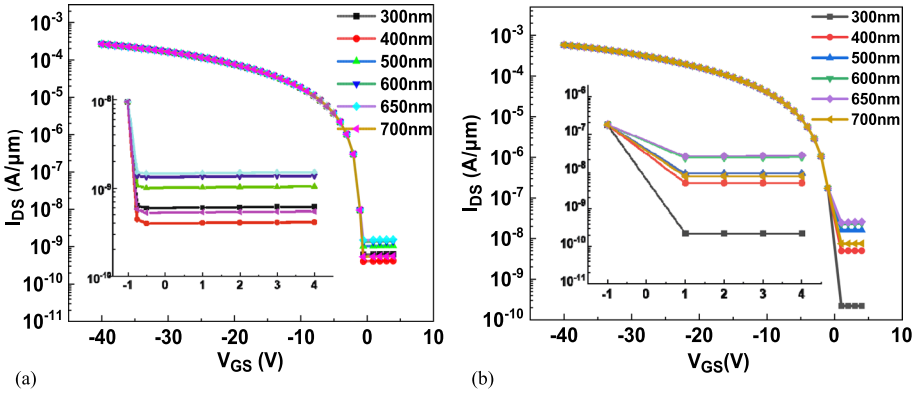

Fig. 10 **a** and **b** showing the variation in drain current versus gate voltage at constant Vds of − 40 V for different wavelengths of applied light bias of 1W/cm^2 in SG-OPT and DG-OPT respectively

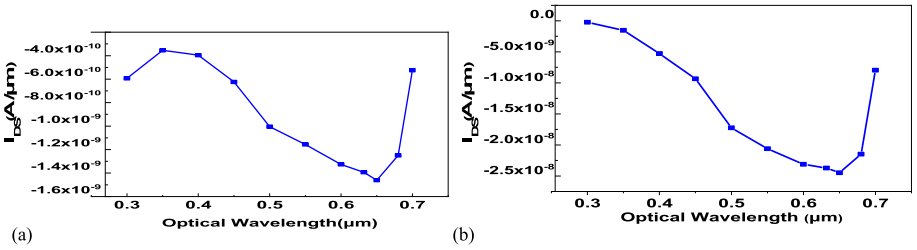

Fig. 11 **a** and **b** Spectral Response of SG-OPT and DG-OPT respectively shows the variation drain current with the applied optical wavelengths at no gate bias condition in SG-OPT

considered as hindrance in the OFET's but these traps can be manipulated in subthreshold region to create energy barrier which helps with the dissociation of excitions and generation of free carriers in the device (Klauk 2010). Moreover the photo-generated electrons gets trapped in the oxide semiconductor interface, which in turn can create a shift in required threshold voltage by causing the device to inject and accumulate more majority carriers i.e. holes in the channel (Sangeeth et al. 2010). However the shift in the threshold voltage is unnoticeable as the trapped electrons aren't sufficient to create a shift and thus photovoltaic effect is not dominant in the results.

The transfer characteristics of both the OPT's are measured for a range of spectral wavelengths and at beam intensity of 1 W/cm^2 is shown in the Fig. 9. As the wavelength of an incident optical light does impact the various performance characteristics of the device. From the Fig. 10a and b it is quit evident at 650 nm both the OPT's are working more efficiently than other wavelengths.

Spectral characteristics of the photosensitive single gate and dual gate Pentacene based OPT's are obtained under the light intensity of 1 W/cm^2 when no gate bias is applied and Vds is − 40 V as shown in Fig. 11. It is measured to find out the optimum wavelength for maximum photo-absorption and photodetection. At 650 nm drain current value of DG-OPT is 2.5×10^{-8} which is much more than the value of SG-OPT. It is clear

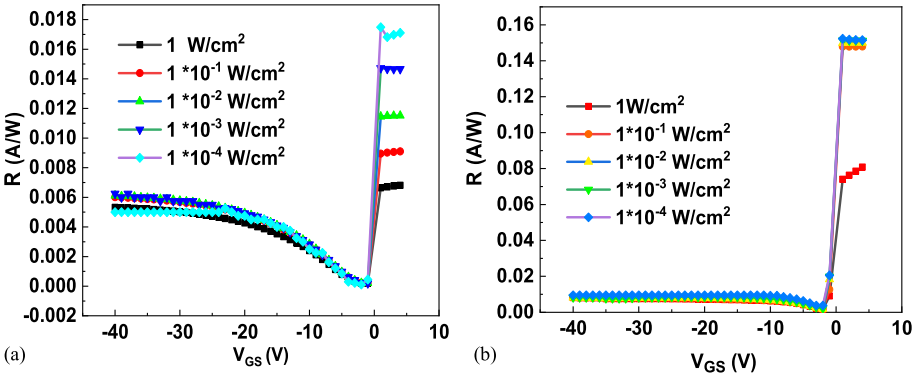

Fig. 12 **a** and **b** showing the variation in photoresponsivity of simulated SG-OPT and DG-OPT when the applied with gate and different light bias with wavelength of 650 nm at constant Vds of − 40 V respectively

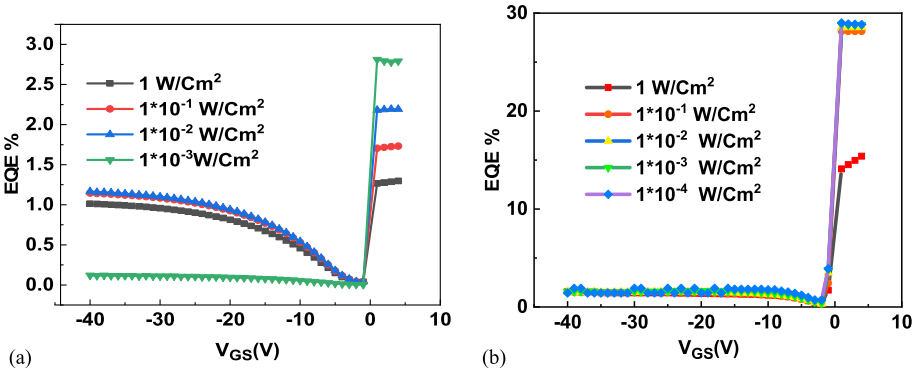

Fig. 13 **a** and **b** EQE variation with applied gate bias at at different light bias with wavelength of 650 nm and constant VDS = − 40 V for SG-OPT and DG-OPT

from this characteristics pentacene based SG-OPT and DG-OPT works more efficiently in 300 nm-700 nm wavelength range i-e visible range, more particularly at 650 nm.

Figure 12a and b shows the photoresponsivity curve of the OPT's when exposed to monochromatic source of different beam intensities with wavelength of 650 nm. So clearly with increase in beam intensity photoresponsivity decreases because the electrons generated at low light intensities acquire the deep trap states that will take extensively have large recombination lifetimes whereas electrons generated at high irradiances fill shallower trap states with shorter recombination lifetime. (Xu et al. 2013) Additionally responsivity of DG-OPT is 0.16 (A/W) which is double the value of SG-OPT in photoconductive mode when light bias of 1 W/cm^2 is applied, it can be credited to the interfacial traps near both the top and bottom sides of channel.

Figure 13a and b showing the EQE variation, the responsivity and External quantum efficiency is interrelated to each other. The observed EQE in photoconductive mode when both the OPT's are applied with light bias of 1W/cm^2, DG-OPT is 30% and SG-OPT is 3%.

The Photosensitivity of OPT's are calculated to determine the degree of sensitivity of OPT's when applied with the light bias. Figure 14 showed the variation of

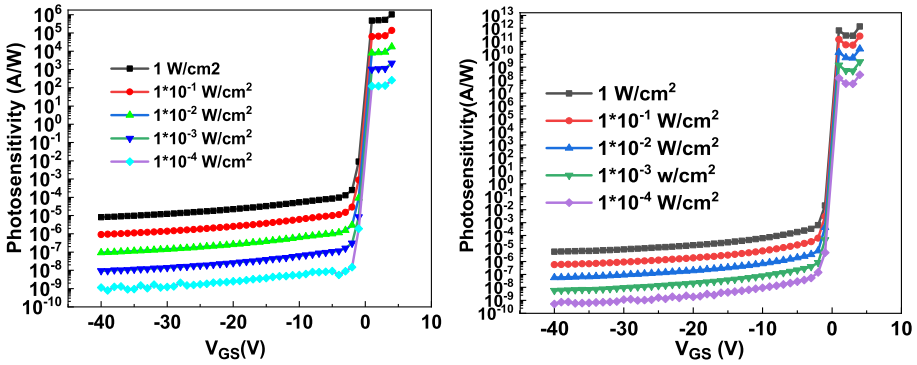

Fig. 14 **a** and **b** showing the variation in the photosensitivity with applied gate bias and with different light bias with wavelength of 650 nm and at constant Vds of − 40 V in SG-OPT and DG-OPT respectively

photosensitivity in both depletion mode and accumulation mode, with the application of different intensities of light of 650 nm wavelength.It is clearly evident from the given characteristics photosensitivity increases with increase in light bias. As the dark current in Depletion Mode of DG-OPT is very low as compared to SG-OPT due to the traps present near both the primary and secondary gate and semiconductor interface, the interfacial traps are manipulated in subthreshold region that is responsible for the higher photosensitivity in DG-OPT. As with increase in light bias more carriers will be generated thus the difference of dark current and photocurrent increase which increases in photosensitivity of device. The DG-OPT shows higher sensitivity with order of 10^{12} as compared to the SG-OPT which shows photosensitivity of order 10^{6} in photoconductive mode when applied with light bias of 1W/cm^2. Also it can be credited to the configurational differences of the two OPT's and interfacial trap manipulation.

4 Conclusion

In this work, we have studied two dimensional optoelectronic simulation of single gate and dual gate pentacene based Organic Photo transistors. We have emphasized on the variation of essential figures of merit while evaluating the progress of these configurations. This study shows how these different configurational OPT designs can influence the essential performance parameters while observing the variations in drain current, Current density, Energy band Diagrams and the various essential performance parameters such as Responsivity, photosensitivity, spectral response, quantum efficiency etc.The essential parameter's such as Photosensitivity, responsivity, EQE, photosensitivity of DG-OPT was observed to be double of the value of SG-OPT. This study shows that DG-OPT makes a viable applicant for light sensing applications.

Author Contributions IB: Simulation, Computation, TCAD software and Writing—Original draft preparation. SIA: Conceptualization, Computation, TCAD software, Revision, Supervision, and Validation. LM: Computation, TCAD software Simulation and Writing. ZR: Simulation and Writing. SA: Revision, Supervision, and Validation.

Funding The authors declare that no funds, grants, or other support received during the preparation of this manuscript.

Data availability Not Applicable.

Declarations

Conflicts of interest The authors declare no conflict of interest.

Ethical approval Not Applicable.

Consent for publication Not Applicable.

Informed consent Not Applicable.

Research involving human participants and/or animals Not Applicable.

References

Baeg, K.J., Binda, M., Natali, D., Caironi, M., Noh, Y.Y.: Organic light detectors: photodiodes and phototransistors. Adv. Mater. **25**(31), 4267–4295 (2013). https://doi.org/10.1002/adma.201204979

Bhargava, K., Bilgaiyan, A., Singh, V.: Two dimensional optoelectronic simulation based comparison of top and bottom contact organic phototransistors. J. Nanosci. Nanotechnol. **15**(12), 9414–9422 (2015). https://doi.org/10.1166/jnn.2015.10737

Chen, Q., Lai, D., He, L., Yan, Y., Li, E., Liu, Y., Zeng, H., Chen, H., Guo, T.: High-Performance vertical organic phototransistors enhanced by ferroelectrics. ACS Appl. Mater. Interfaces **13**(1), 1035–1042 (2020). https://doi.org/10.1021/acsami.0c18281

Chou, H.-H., Nguyen, A., Chortos, A., To, J.W., Lu, C., Mei, J., Kurosawa, T., Bae, W.-G., Tok, J.B.-H., Bao, Z.: A chameleon-inspired stretchable electronic skin with interactive colour changing controlled by tactile sensing. Nat. Commun. **6**(1), 1–10 (2015). https://doi.org/10.1038/ncomms9011

Chow, P.C., Matsuhisa, N., Zalar, P., Koizumi, M., Yokota, T., Someya, T.: Dual-gate organic phototransistor with high-gain and linear photoresponse. Nat. Commun. **9**(1), 4546 (2018). https://doi.org/10.1038/s41467-018-06907-6

Chow, P.C., Someya, T.: Organic photodetectors for next-generation wearable electronics. Adv. Mater. **32**(15), 1902045 (2020). https://doi.org/10.1002/adma.201902045

Haneef, H.F., Zeidell, A.M., Jurchescu, O.D.: Charge carrier traps in organic semiconductors: a review on the underlying physics and impact on electronic devices. J. Mater. Chem. C **8**(3), 759–787 (2020)

Hu, L., Pasta, M., La Mantia, F., Cui, L., Jeong, S., Deshazer, H.D., Choi, J.W., Han, S.M., Cui, Y.: Stretchable, porous, and conductive energy textiles. Nano Lett. **10**(2), 708–714 (2010). https://doi.org/10.1021/nl903949m

Hwang, G.T., Byun, M., Jeong, C.K., Lee, K.J.: Flexible piezoelectric thin-film energy harvesters and nanosensors for biomedical applications. Adv. Healthcare Mater. **4**(5), 646–658 (2015). https://doi.org/10.1002/adhm.201400642

Kim, D.-H., Lu, N., Ma, R., Kim, Y.-S., Kim, R.-H., Wang, S., Wu, J., Won, S.M., Tao, H., Islam, A.: Epidermal electronics. Science **333**(6044), 838–843 (2011). https://doi.org/10.1126/science.1206157

Klauk, H.: Organic thin-film transistors. Chem. Soc. Rev. **39**(7), 2643–2666 (2010). https://doi.org/10.1039/B909902F

Klauk, H., Zschieschang, U., Halik, M.: Low-voltage organic thin-film transistors with large transconductance. J. Appl. Phys. **10**(1063/1), 2794702 (2007)

Lee, W.H., Choi, H.H., Kim, D.H., Cho, K.: 25th anniversary article: microstructure dependent bias stability of organic transistors. Adv. Mater. **26**(11), 1660–1680 (2014). https://doi.org/10.1002/adma.201304665

Li, Q., Guo, Y., Liu, Y.: Exploration of near-infrared organic photodetectors. Chem. Mater. **31**(17), 6359–6379 (2019). https://doi.org/10.1021/acs.chemmater.9b00966

Liguori, R., Sheets, W., Facchetti, A., Rubino, A.: Light-and bias-induced effects in pentacene-based thin film phototransistors with a photocurable polymer dielectric. Org. Electron. **28**, 147–154 (2016). https://doi.org/10.1016/j.orgel.2015.10.029

Mittal, P., Kumar, B., Negi, Y.S., Kaushik, B.K., Singh, R.: Channel length variation effect on performance parameters of organic field effect transistors. Microelectron. J. **43**(12), 985–994 (2012). https://doi.org/10.1016/j.mejo.2012.07.016

Nishide, H., Oyaizu, K.: Toward flexible batteries. Science **319**(5864), 737–738 (2008). https://doi.org/10.1126/science.1151831

Noh, Y.-Y., Kim, D.-Y., Yase, K.: Highly sensitive thin-film organic phototransistors: Effect of wavelength of light source on device performance. J. Appl. Phys. **98**(7), 074505 (2005). https://doi.org/10.1063/1.2061892

Ren, H., Chen, J.D., Li, Y.Q., Tang, J.X.: Recent progress in organic photodetectors and their applications. Adv. Sci. **8**(1), 2002418 (2021). https://doi.org/10.1002/advs.202002418

Salvatore, G.A., Münzenrieder, N., Kinkeldei, T., Petti, L., Zysset, C., Strebel, I., Büthe, L., Tröster, G.: Wafer-scale design of lightweight and transparent electronics that wraps around hairs. Nat. Commun. **5**(1), 1–8 (2014)

Sangeeth, C.S., Stadler, P., Schaur, S., Sariciftci, N., Menon, R.: Interfaces and traps in pentacene field-effect transistor. J. Appl. Phys. **108**(11), 113703 (2010). https://doi.org/10.1063/1.3517085

Sirringhaus, H.: Device physics of solution-processed organic field-effect transistors. Adv. Mater. **17**(20), 2411–2425 (2005). https://doi.org/10.1002/adma.200501152

Someya, T., Dodabalapur, A., Huang, J., See, K.C., Katz, H.E.: Chemical and physical sensing by organic field-effect transistors and related devices. Adv. Mater. **22**(34), 3799–3811 (2010). https://doi.org/10.1002/adma.200902760

Tavasli, A., Gurunlu, B., Gunturkun, D., Isci, R., Faraji, S.: A review on solution-processed organic phototransistors and their recent developments. Electronics **11**(3), 316 (2022). https://doi.org/10.3390/electronics11030316

Torsi, L., Magliulo, M., Manoli, K., Palazzo, G.: Organic field-effect transistor sensors: a tutorial review. Chem. Soc. Rev. **42**(22), 8612–8628 (2013). https://doi.org/10.1021/acssensors.0c00694

Xu, H., Li, J., Leung, B.H., Poon, C.C., Ong, B.S., Zhang, Y., Zhao, N.: A high-sensitivity near-infrared phototransistor based on an organic bulk heterojunction. Nanoscale **5**(23), 11850–11855 (2013). https://doi.org/10.1039/C3NR03989G

Yamashita, Y.: Organic semiconductors for organic field-effect transistors. Sci. Technol. Adv. Mater. **10**(2), 024313 (2009). https://doi.org/10.1088/1468-6996/10/2/024313

Yu, H., Bao, Z., Oh, J.H.: High-performance phototransistors based on single-crystalline n-channel organic nanowires and photogenerated charge-carrier behaviors. Adv. Func. Mater. **23**(5), 629–639 (2013). https://doi.org/10.1002/adfm.201201848